THEORETICAL MODELING OF TRACTION CHARACTERISTICS BETWEEN PAPER-WEB AND STEEL-ROLLER BASED ON THE CONTACT MECHANICS

By

H. Hashimoto
Tokai University
JAPAN

ABSTRACT

This report describes the theoretical modeling of friction coefficient between uncoated paper web (newsprint; for example) and steel roller. In the modeling, the paper base is approximated by the linear spring and surface asperities are treated as rigid body. Introducing the contact mechanics and assuming the Gaussian distribution of surface asperities, the mixed friction coefficient is formulated theoretically for a wide range of roller surface velocity, in which the air film thickness between the web and roller is estimated based on the foil bearing model. In the experiments, the newsprint is used as uncoated paper-web. Euler's belt formula is applied to calculate the friction coefficient from the measured data on tension increase. The measurements are carried out by changing five design parameters such as web width, wrap angle, tension, roller diameter, and roller surface velocity. The measured results are compared with the predicted results by the friction model. Good agreements can be seen between the predicted results and measured results.

NOMENCLATURES

A_a : apparent contact area [m^2]
A_r : real contact area [m^2]
B : web wrap angle [rad]
C : experimental constant [m/s]
E_a : Young's modulus of asperity [GPa]
E_b : Young's modulus of web in web thickness direction [GPa]
E_c : Young's modulus of web in cross direction [GPa]
E_m : Young's modulus of web in machine direction [GPa]
h : web spacing (air film thickness) [m]
k : permeability [m^2]
L : web width [m]
p_a : ambient pressure [Pa]

p_c : averaged contact pressure [Pa]
$\bar{p}$: averaged pressure due to applied load (=T/R) [Pa]
R : roller radius [m]
T : web tension [N/m]
ΔT : tension increase [N/m]
t : time [s]
t_b : web thickness [m]
U : total velocity (= U_r+U_w)[m/s]
U_r : roller velocity [m/s]
U_w : web velocity [m/s]
W : Load applied [N]
W_c : Load supported by asperities [N]
W_f : Load supported by air film [N]
x : coordinate in the web transportation direction [m]
x_e : outlet position of web wrap region [m]
x_s : intlet position of web wrap region [m]
z : coordinate in the cross direction or web thickness direction [m]
ε : web speed parameter (=$6\eta U/T$)
$\phi(z)$: probability density
η : air film viscosity [Pa·s] or surface asperity density [m^{-2}]
χ : web permeable parameter (=$kTB/(\eta t_w RU)$)
χ_c : load ratio supported by contact pressure
χ_f : load ratio supported by air film pressure
λ : web width parameter (=$L/(2R\varepsilon^{1/3})$)
μ : friction coefficient
μ_c : friction coefficient due to asperity contact
μ_{cc} : experimental constant
μ_f : friction coefficient due to air film flow
σ : composite RMS roughness (=$(\sigma_r^2+ \sigma_w^2)^{1/2}$) [m]
σ_r : RMS roughness of roller surface [m]
σ_w : RMS roughness of web surface [m]

INTRODUCTION

A web is continuous, thin and very flexible material transported by the traction between the web and roller under tension through various processes including printing, recording, coating, drying, laminating, etc. prior to being converted to final products. The web processing systems are widely seen in many industrial fields such as paper making, newsprinting, thin metal forming, textile, magnetic tape manufacturing and so on. In such systems, the moving web and the rotating roller bring the surround air between the web and roller due to viscosity. As a result, the web-roller interface behaves as the self-acting foil bearings, and it causes a decrease of traction between the web and roller. Increasing the air film thickness more than the asperity heights of the web and roller surfaces, the available traction is nothing more than the air film friction which is actually equivalent to near zero-friction. In the case of the idler roller driven by web, for example, an insufficient traction results in lower speed of roller than the web and then reduces the tracking ability of web which causes finally the web defects. As a decrease in traction is a direct result of air entrainment between the web and roller, it is important to understand

the traction characteristics between the web and roller including the effects of air film for controlling the traction suitably in many web applications. However, the references on the traction characteristics between the web and roller in web handling processes are very limited.

Knox and Sweency examined the effect of the entrained air on the traction between a web and a stationary roller [1], in which the air film thickness was modeled using the foil bearing equation by Eshel and Elrod [2] which is derived by treating the web as an infinitely wide membrane and the air film using a simplified Reynolds equation where air compressibility is neglected. The contact between web and roller, which typically occurs at asperities on the surfaces, was not modeled. Ducotey and Good [3] conducted an extensive parameter study on traction. All data was referenced to a single curve because of an additional normal force caused by electrostatic effects. Therefore, the study only showed the relative effects of the parameters tested. Moreover, Ducotey and Good [4] developed for predicting traction in web handling applications and showed experimentally the applicability of the algorithm for newsprint and PET, permeable and impermeable webs, respectively. Rice, Muftu and Cole [5] studied experimentally and theoretically the traction developed between impermeable web and a nonvented rotating steel roller. The traction tests were conducted for a series of eight impermeable webs representing a wide range of surface roughness characteristics. Hashimoto [6] presented the simple formula for predicting the air film thickness between the impermeable web and steel roller based on the numerical solutions, and then Hashimoto and Nakagawa [7] extended the model to estimate the friction coefficient between the impermeable web and nonvented or vented steel roller.

In this paper, the theoretical model for estimating the friction coefficient between the steel roller and paper-web is quite newly formulated based on the contact mechanics. The predicted results are compared with the measured ones, and the applicability of the model and the effects of operation parameters on the traction characteristics are clarified.

THEORETICAL MODELING

Surface topography of paper-web

Figure 1 shows an example of a web transport system, in which the moving web is supported by several kinds of rollers. In such a transport system, it is very important to understand the traction characteristics between the web and roller. The friction coefficient between the web and roller will be changed greatly due to the web spacing, and the web spacing strongly depends on the web wrap angle, width, tension, roller diameter etc. Figure 2 shows the relation among these quantities at the interface between the web and roller. Before making the model for friction coefficient, it is necessary to examine the surface topography of web and roller. In the observation of surface topography, the co-focused laser microscope is used. Figure 3 shows the top view and side view of the uncoated paper (newsprint) obtained by the co-focused laser microscope, and Table 1 shows the physical properties of the uncoated paper. From Figure 3 and Table 1, it follows that the uncoated paper is recognized as 3-dimentional nonuniform material and it is mainly deformable in the thickness direction. Therefore, the basical part of web is modeled by the thickness directional spring. The web surfaces is curved with fiber-like hard asperities and the Young's modulus of the asperities E_a is much larger than the modulus in the machine direction E_m, cross direction E_c or web thickness direction E_b, and then the asperities can be modeled by the rigid body.

From the observed data by co-focused laser microscope, the roughness curve as shown in Figure 4 is also obtained, and then the probability density of asperity height of

paper-web surface is calculated as the plotted data in Figure 5. As can be seen in Figure 5, the probability density is approximated by the Gaussian distribution curve given as:

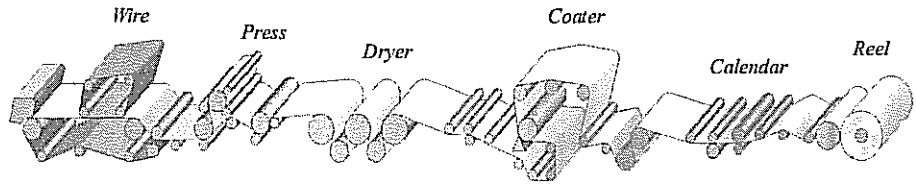

Figure 1 – Papermaking machine

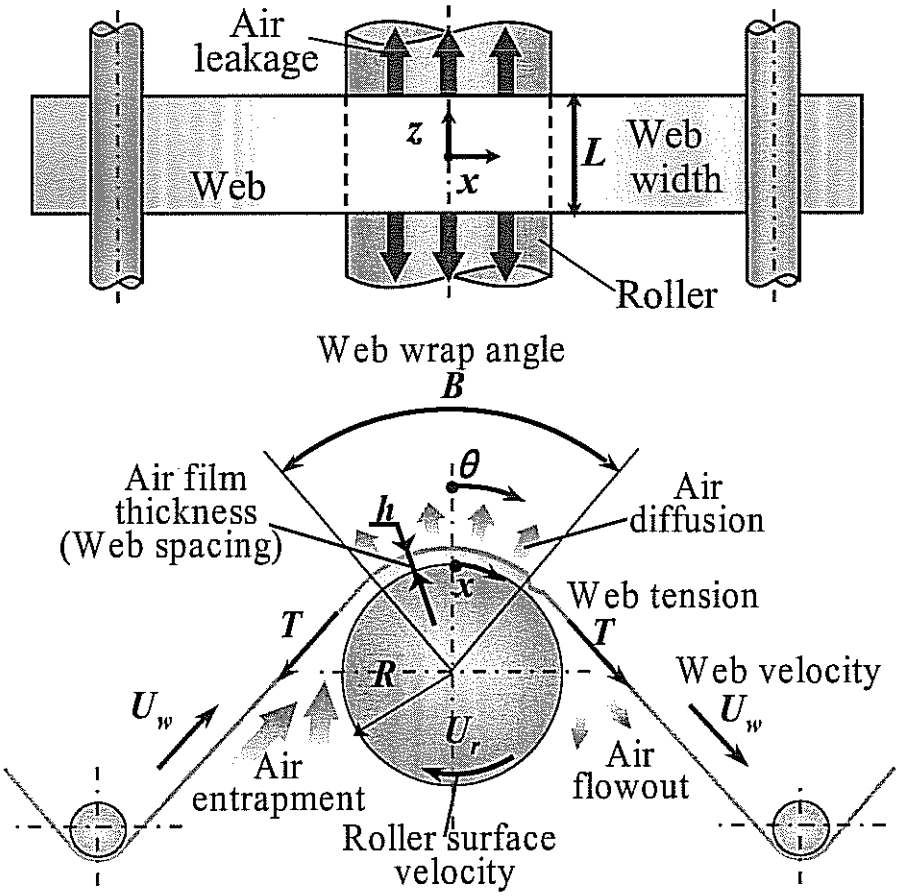

Figure 2 – Interface model between web and roller

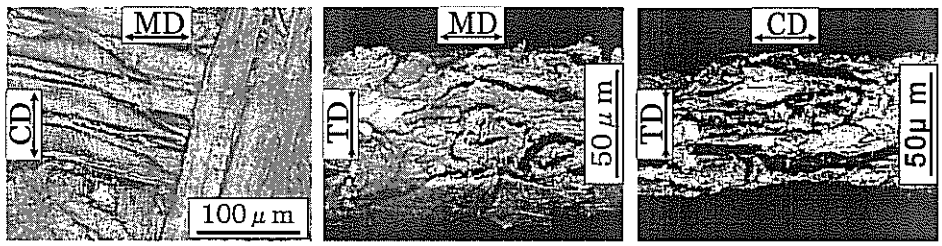

(a) Top (b) Side (MD) (c) Side (CD)

Figure 3 – Top and side view of uncoated

Table1 Physical properties of uncoated paper

Item	Measured value	Item	Measured value
Young's modulas of web in thickness direction	E_t=175 kPa	Young's modulas of web surface asperity	E_h=40 GPa
Young's modulas of web in machine direction	E_m=4.46 GPa	RMS roughness of web	σ_w=4.0 μm
		R_a roughness of web surface	R_a=2.39 μm
		R_{max} roughness of web	R_{max}=27.6 μm
Young's modulas of web in cross direction	E_c=1.66 GPa	Web thickness	t_b=70 μm
		Web permeability	$k=5\times10^{-15}$ m^2

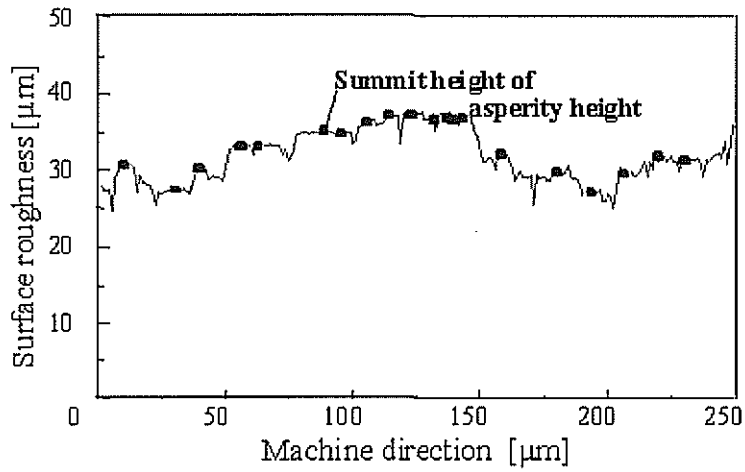

Figure 4 – Surface roughness curve

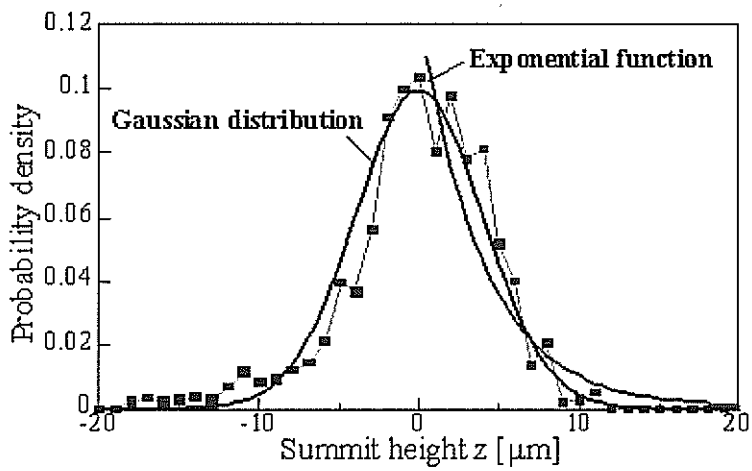

Figure 5 – Probability density of asperity height

$$\phi_1(z) = \frac{1}{\sigma_w \sqrt{2\pi}} \exp\left(-\frac{z^2}{2\sigma_w{}^2}\right) \tag{1}$$

or by the more simple exponential curve given as :

$$\phi_2(z) = \frac{1}{2\sigma_w} \exp\left(-\frac{z}{\sigma_w}\right) \tag{2}$$

Contact mechanics model between paper-web and steel roller

Based on the above consideration, the contact mechanics model between paper-web and steel roller is expressed schematically as shown in Figure 6, in witch as the roller surface roughness σ_r is much smaller than the web surface roughness σ_w, σ_r is neglected.

From Figure 6, the elastic deformation of i-th asperity due to contact δ_i is given by:

$$\delta_i = z - h \tag{3}$$

On the other hand, following Fooke's low, δ_i is expressed as:

$$\delta_i = \frac{t_b}{E_b} \frac{W_{ci}}{A_{ai}} \tag{4}$$

where A_{ai} means apparent contact area of i-th asperity.

The asperity density is defined as:

$$\eta = \frac{N}{A_a} \tag{5}$$

Then, the apparent contact area of i-th asperity is given by:

$$A_{ai} = \frac{A_a}{N} = \frac{1}{\eta} \tag{6}$$

From Eqs.(3),(4) and (6), the contact load to i-th asperity is :

$$W_{ci} = \frac{1}{\eta}\frac{E_b}{t_b}(z-h) \tag{7}$$

As a result, the expected value of total contact load supported by asperities is obtained as follows:

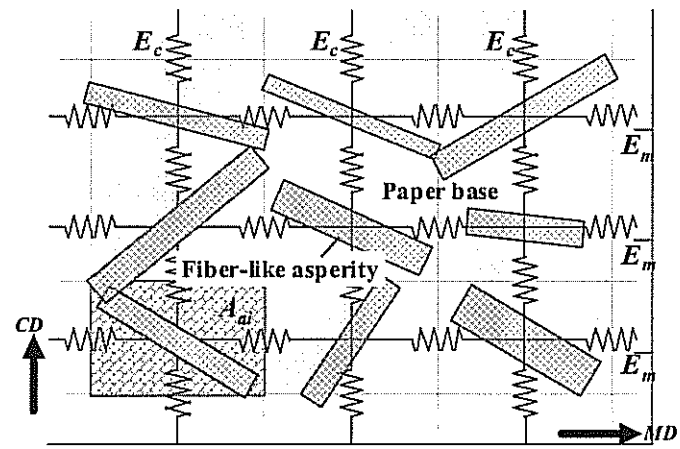

(a) Top view

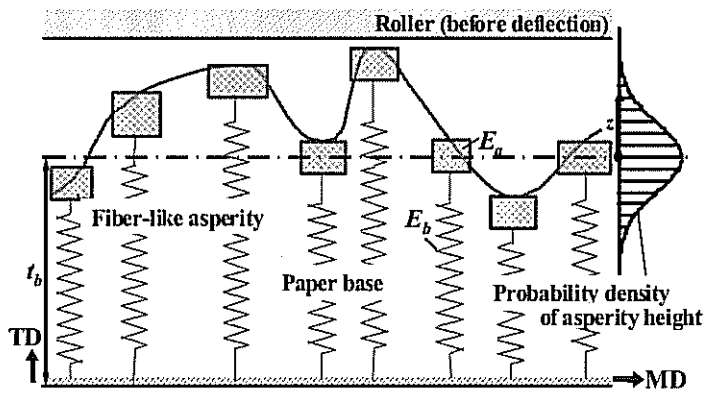

(b) Side view

Figure 6 – Contact model between paper-web and steel roller

$$W_c = N\int_h^\infty W_{ci}\phi_1(z)dz \cong \frac{1}{\eta}\frac{E_b}{t_b}\int_h^\infty (h-z)\phi_2(z)dz \tag{8}$$

Using Eqs. (2) and (5), the total contact load is finally expressed as:

$$W_c = \frac{A_a E_b \sigma_w}{2t_b} \exp\left(-\frac{h}{\sigma_w}\right) \tag{9}$$

The averaged contact pressure between paper-web and steel roller is given as follows:

$$p_c = \frac{W_c}{A_a} = \frac{E_b \sigma_w}{2t_b} \exp\left(-\frac{h}{\sigma_w}\right) \tag{10}$$

Figure 7 shows the variation of the averaged contact pressure p_c with web spacing (air film thickness) h. The contact pressure decreases rapidly with an increase of the spacing h, and it actually disappears when the spacing h becomes larger than $3\sigma_w$.

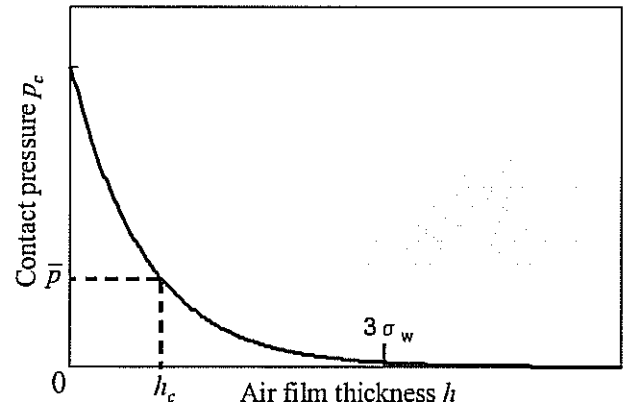

Figure 7 – Relation between averaged contact pressure and air film thickness.

Now, lets define the spacing h_c which is equivalent to the spacing under the condition of $p_c = \bar{p} = T/R$.

From Eq.(10), the spacing h_c is evaluated as:

$$h_c = \sigma_w \ln\left(\frac{E_b \sigma_w}{2t_b \bar{p}}\right) \tag{11}$$

When the spacing h is smaller than h_c, $h < h_c$, the total load W is actually supported by the asperity contact pressure p_c only, and such a condition is recognized as the "boundary lubrication condition ". On the other hand, when the spacing h is larger than $3\sigma_w$, $h > 3\sigma_w$, the total load W is actually supported only by the air film pressure p_f generated in the spacing, and such a condition is recognized as the "fluid film lubrication condition". Moreover, when the spacing h is larger than h_c and smaller than $3\sigma_w$, $h_c <$

$h<3\sigma_w$, the total load W is supported by both the asperity contact pressure p_c and air film pressure p_f, and such a condition is recognized as the "mixed lubrication condition".

The load ratio supported by the asperity contact pressure, χ_c, is defined as:

$$\chi_c = \frac{W_c}{W} = \frac{p_c A_a}{\bar{p} A_a} = \frac{p_c}{\bar{p}} \tag{12}$$

Substituting Eq.(10) into Eq.(12) and considering that the total load is actually supported by the asperity contact pressure only for $h< h_c$, the ratio χ_c is obtained as follows:

$$\chi_c = \begin{cases} 1 & (h < h_c) \\ \dfrac{E_b \sigma_w}{2 t_b \bar{p}} \exp\left(-\dfrac{h}{\sigma_w}\right) & (h_c \le h \le 3\sigma_w) \\ 0 & (h > 3\sigma_w) \end{cases} \tag{13}$$

The load ratio supported by the air film pressure, χ_f, is then defined as :

$$\chi_f = 1 - \chi_c \tag{14}$$

Figure 8 shows the relation between the ratio χ_c, χ_f and the spacing h according to three types of lubrication conditions discussed above.

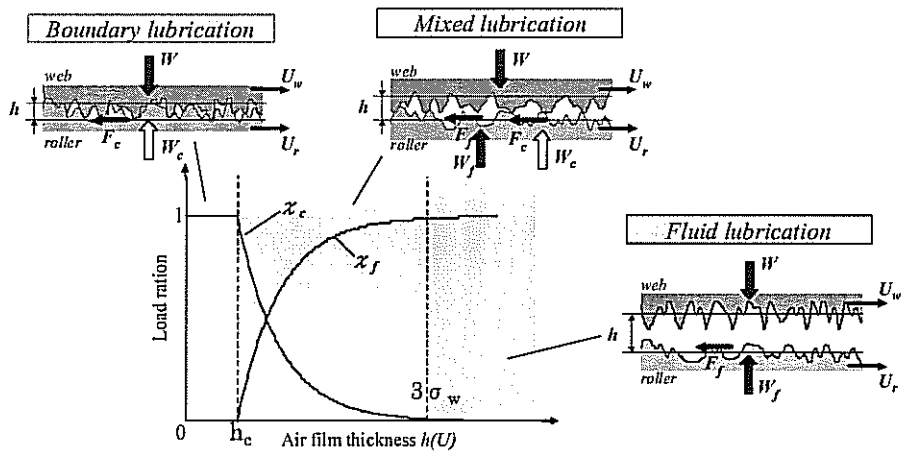

Figure 8 – Relation between load ratio and air film thickness

Evaluation of web spacing

The foil bearing model, as shown in Figure 2, is generally applied to evaluate the web spacing h in the web wrapped region, in which the air film pressure and the spacing are obtained theoretically by solving the following modified Reynolds equation and web equilibrium equation simultaneously [7].

$$\frac{\partial}{\partial x}\left(h^3 p_f \frac{\partial p_f}{\partial x}\right)+\frac{\partial}{\partial z}\left(h^3 p_f \frac{\partial p_f}{\partial z}\right)+\frac{12k}{t_f}p_f(p_f-p_a)=6\eta U\frac{\partial(p_f h)}{\partial x} \tag{15}$$

$$\frac{T}{R}-R\frac{\partial^2 w}{\partial x^2}=\frac{1}{L}\int_{-L/2}^{L/2}(p_f-p_a)dz \tag{16}$$

$$h=w+d \tag{17}$$

$$d=\begin{cases}\dfrac{1}{2R}\left(x+\dfrac{RB}{2}\right)^2 & (x<-\dfrac{RB}{2})\\ 0 & (-\dfrac{RB}{2}\le x\le\dfrac{RB}{2})\\ \dfrac{1}{2R}\left(x-\dfrac{RB}{2}\right)^2 & (x>\dfrac{RB}{2})\end{cases} \tag{18}$$

The boundary conditions for p_f and w are respectively given by:

$$p_f(x_s,z)=p_a, p_f(x_e,z)=p_a \tag{19.a}$$

$$p_f(x,-L/2)=p_a,\ p_f(x,L/2)=p_a \tag{19.b}$$

$$w(x_s)=0,\ w(x_e)=0 \tag{20.a}$$

$$\left(\frac{\partial^2 w}{\partial x^2}\right)_{x=x_s}=0,\quad \left(\frac{\partial^2 w}{\partial x^2}\right)_{x=x_e}=0 \tag{20.b}$$

Following the same manner as has been done by Hashimoto [6], [7], the web spacing h is given finally by the following approximate solution for ®>6 and λ>7.

$$h=\begin{cases}R\varepsilon^{2/3}\left(0.589-\dfrac{1.614}{\lambda}+\dfrac{1.764}{\lambda^2}\right)-R\kappa\left(1+\dfrac{2x}{RB}\right) & (h>0)\\ 0 & (h\le 0)\end{cases} \tag{21}$$

where :

$$\lambda=\frac{L}{2R\varepsilon^{1/3}},\varepsilon=\frac{6\eta U}{T},\kappa=\frac{kTB}{\eta t_f RU},\beta=\frac{B}{\varepsilon^{1/3}} \tag{22}$$

Friction model between paper-web and roller

From Figure 8, the force balance equations in the normal and tangential directions are given respectively as follows:

$$F=F_c+F_f \tag{23}$$

$$W=W_c+W_f \tag{24}$$

Dividing Eqs.(23) and (24) by the total load W, the following equations are obtained.

$$\mu = \frac{F_c}{W} + \frac{F_f}{W} = \frac{F_c}{W_c}\frac{W_c}{W} + \frac{F_f}{W_f}\frac{W_f}{W} \tag{25}$$
$$= \mu_c \chi_c + \mu_f \chi_f$$

$$\chi_c + \chi_f = 1 \tag{26}$$

where the friction coefficients μ_c and μ_f are defined respectively by:

$$\mu_c = \frac{F_c}{W_c}, \mu_f = \frac{F_f}{W_f} \tag{27}$$

Substituting Eq.(13) into Eq.(25) and considering the relation in Eq.(14) or Eq.(26), the effective friction coefficient μ is obtained finally as follows:

$$\mu = \begin{cases} \mu_c & (h < h_c) \\ \mu_c \dfrac{E_b \sigma_w}{2 t_b \bar{p}} \exp\left(-\dfrac{h}{\sigma_w}\right) + \mu_f \left\{1 - \dfrac{E_b \sigma_w}{2 t_b \bar{p}} \exp\left(-\dfrac{h}{\sigma_w}\right)\right\} & (hc \le h \le 3\sigma_w) \\ \mu_f & (h > 3\sigma_w) \end{cases} \tag{28}$$

where μ_c is given by :

$$\mu_c = \begin{cases} \dfrac{2}{\pi} \mu_{cc} \tan^{-1}\left(\dfrac{U}{c}\right) & (h < h_c) \\ \mu_{cc} & (h_c \le h \le 3\sigma_w) \end{cases} \tag{29}$$

and μ_f is given by :

$$\mu_f = \frac{\eta R U}{h T} \tag{30}$$

In Eq.(29), the constants μ_{cc} and C should be determined experimentally by the standard test. In this case, μ_{cc}=0.3, C=0.4 [m/s] were used.

The total effective friction coefficient is calculated as the averaged value of μ in Eq.(28) over the web wrapped region.

MEASUREMENTS

To verify the applicability of Eq.(28) in the web-roller interface problems, the friction coefficient and spacing between the web and roller were measured.

Figure 9 shows the overview of the test rig for measuring the spacing and traction characteristics between the web and roller surfaces. The test rig consists of roller, driven motor, guides, web, weight, speed controller, load cell, optical fiver type gap sensor and

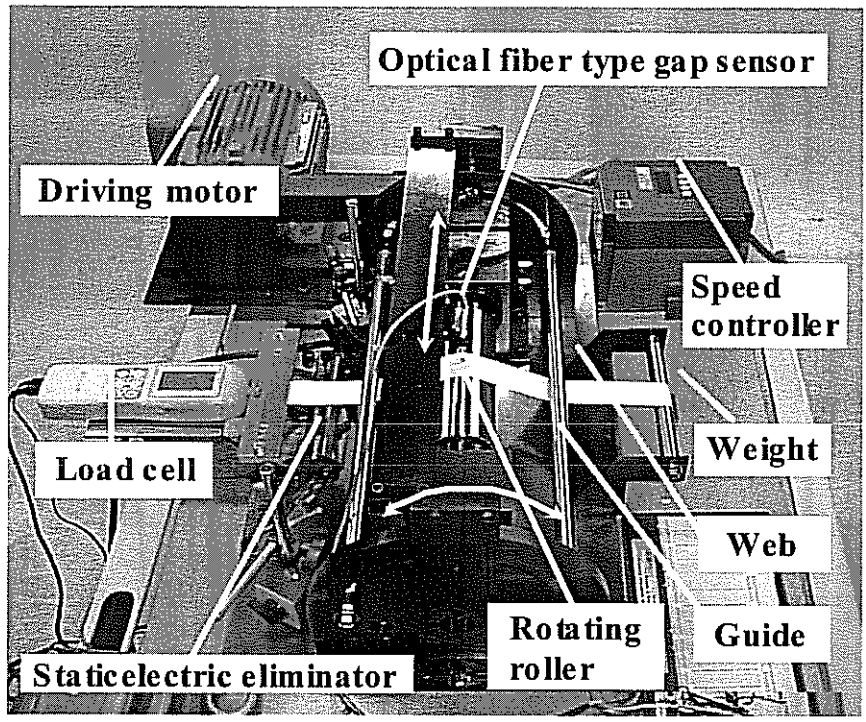

Figure 9 – Overview of test rig

static electricity eliminator. The web is stationary and the roller is rotated by the driving motor. The accuracy of roller rotation is less than 1 μm, and there is minimal effect on the measurements of air film thickness. The wrap angle of the web about the roller, can be changed from 20 deg to 120 deg by adjusting the guides. The web tension is set by varying the dead weight, and the tension increase due to friction between the web and roller surfaces is measured using the load cell. The optical fiber type displacement sensor is used for measuring the air film thickness and the resolution of the sensor is 50 nm. The position of sensor can be changed continuously in both axial and circumferential directions on the rails as shown in Figure 9. But in this measurements, the position was fixed at the central point of web wrapped region. Under the conditions of low relative humidity, the static electricity may affect the measured results, thus during the tests the static electricity eliminator was operated.

After obtaining the tension increase, ΔT, the effective friction coefficient, μ, was calculated by the following Euler's belt formula.

$$\mu = \frac{1}{B} \ln\left(1 + \frac{\Delta T}{T}\right) \tag{31}$$

In the measurements, the five operation parameters, web tension T, wrap angle B, width L, roller radius R and roller surface velocity U, were changed. The measurements were repeated 10 times for each parameter for checking the repeatability. The operation parameters values selected for the measurement are listed in Table 2.

RESULTS AND DISCUSSIONS

The predicted results of friction coefficient between the uncoated paper-web and steel roller by Eq.(28) are compared with the measured data in Figs. 10 through 13, in which the predicted results of web spacing at the inlet, central and exit positions are also indicated by the dashed lines. The solid lines show the predicted results by Eq.(28) and the plots are the averaged values of 10 times measured data. Figure 10 shows the relation between the friction coefficient and roller velocity for changing the web wrap angle.

Table2 Test conditions

Item	Measured value
Roller surface velocity	U_r=0~40 m/s
Web velocity	U_w=0 m/s
Web wrap angle	B=20, 40, 60 deg
Web tension	T=40, 80, 120 N/m
Web width	L=0.020, 0.035, 0.100
Roller radius	R=0.035, 0.055 m
RMS roller surface	σ_r=0.6 μm
Room temperature	23.5 ~ 25.7 °C
Relative humidity	18 ~ 31 %

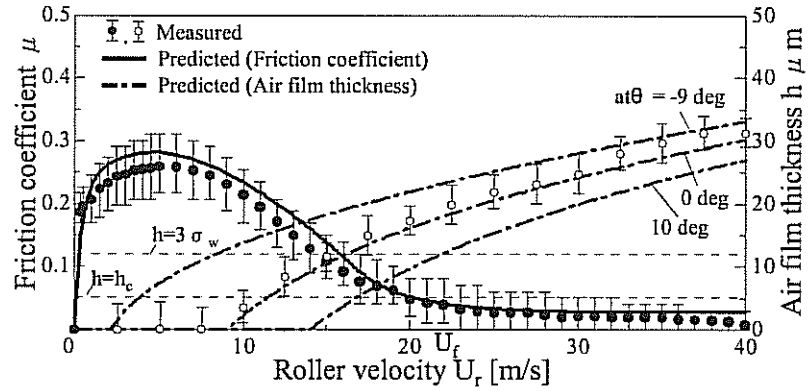

(a) B=20 [deg]

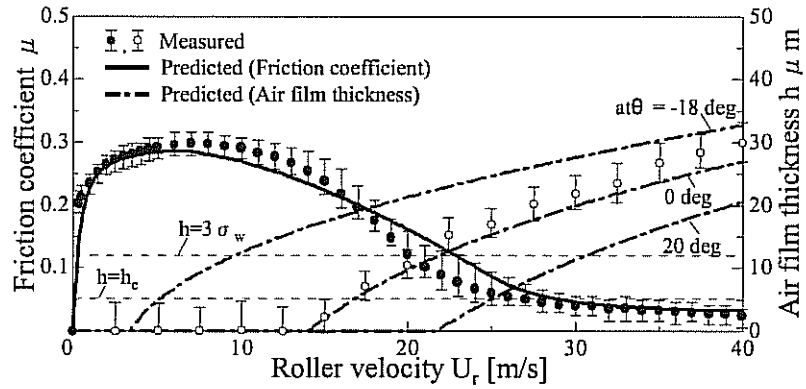

(b) B=40 [deg]

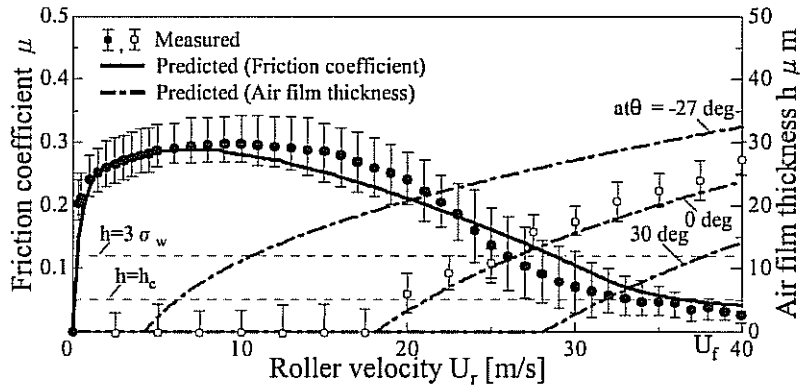

(c) B=60 [deg]

Figure 10 – Variation of friction coefficient with roller velocity as a parameter of web wrap angle
(R=0.055[m], L=0.035[m], T=80[N/m])

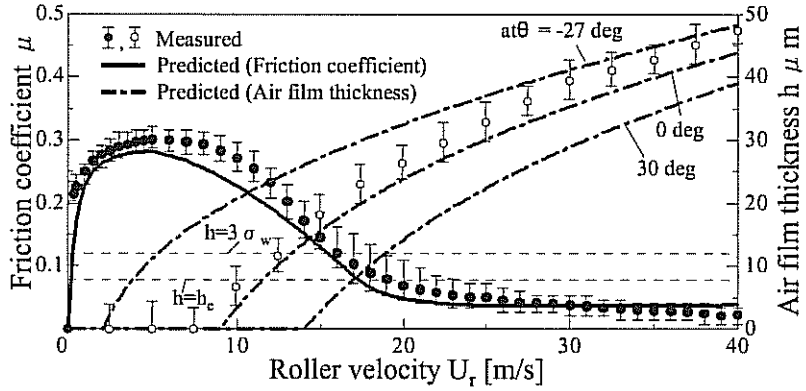

(a) T=40 [N/m] ($\bar{p}$=0.73 [kPa])

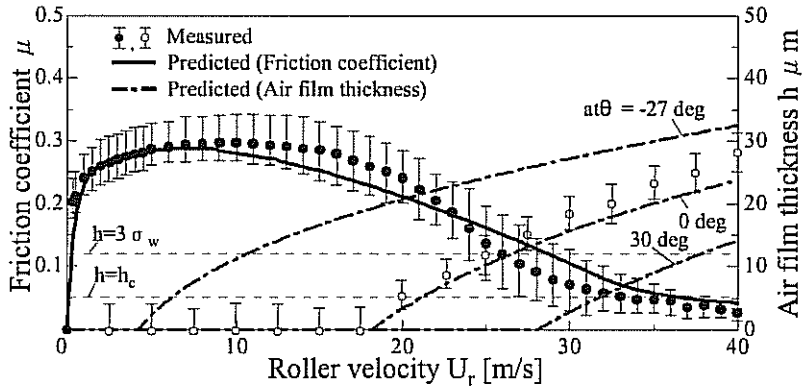

(b) T=80 [N/m] ($\bar{p}$=1.45 [kPa])

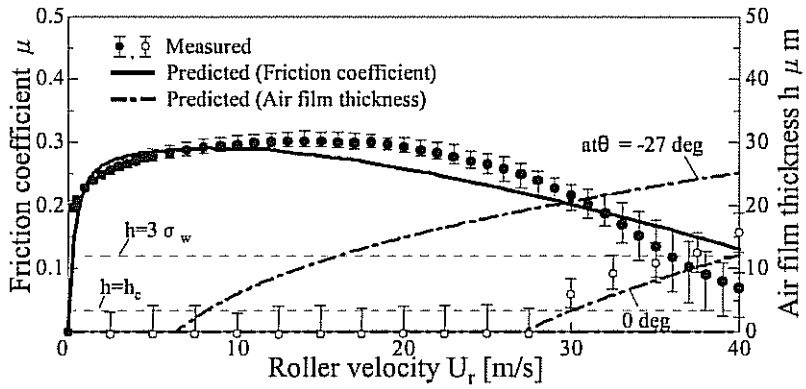

(c) T=120 [N/m] ($\bar{p}$=2.20 [kPa])

Figure 11 –Variation of friction coefficient with roller velocity as a parameter of web tension
(R=0.055[m], L=0.035[m], B=60[deg])

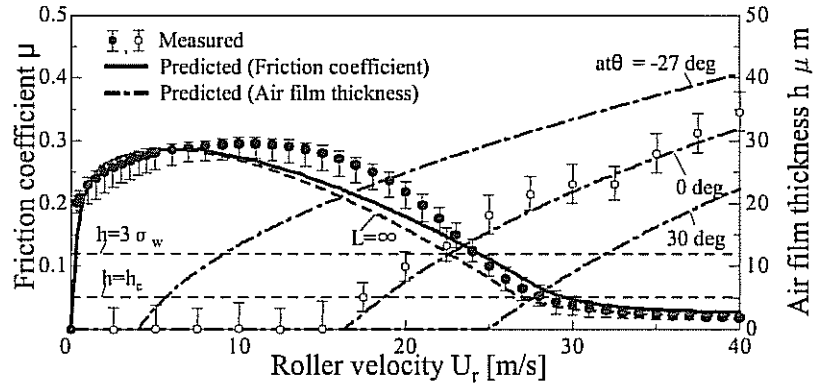

(a) L=0.100 [m]

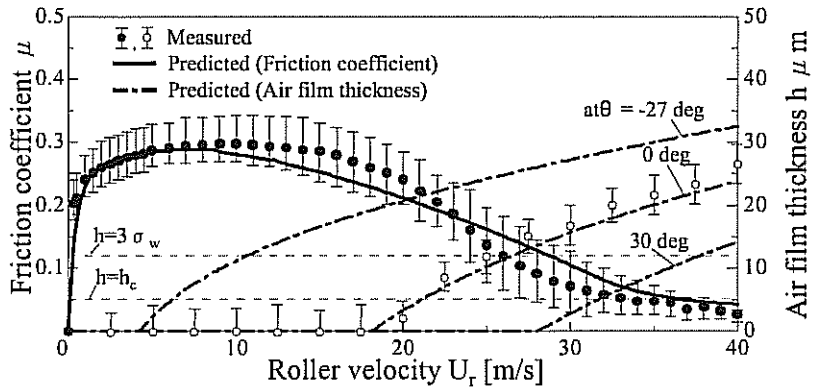

(b) L=0.035 [m]

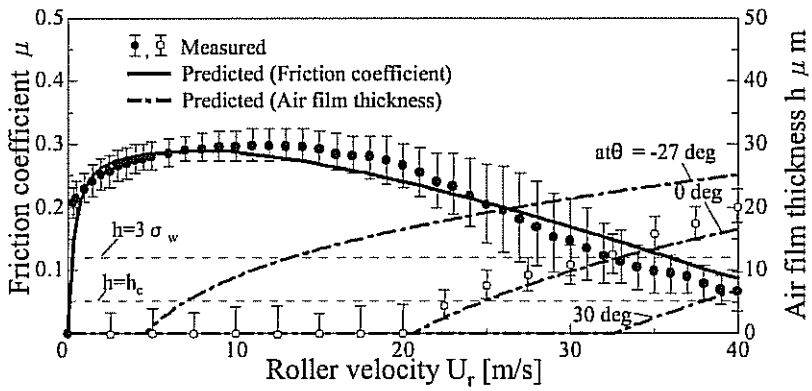

(c) L=0.020 [m]

Figure 12 – Variation of friction coefficient with roller velocity as a parameter of web width
(R=0.055[m], B=60[deg], T=80[N/m])

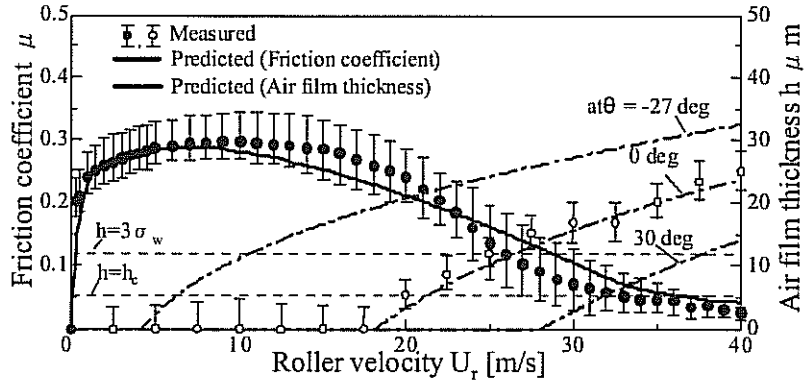

(a) R=0.055 [m]

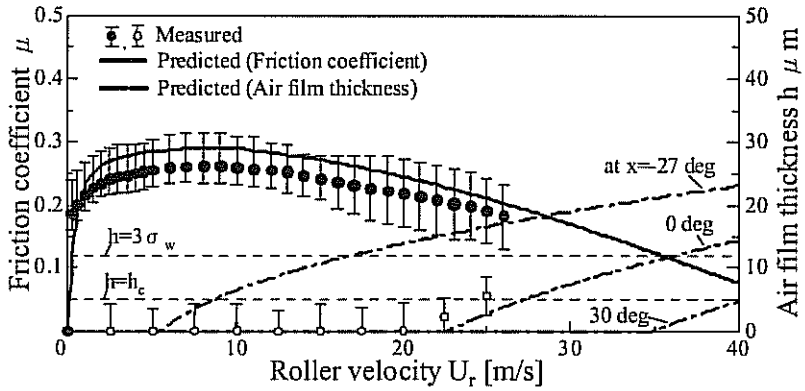

(b) R=0.035 [m]

Figure 13 – Variation of friction coefficient with roller velocity as a parameter of roller radius
(B=60[deg], L=0.035[m], T=80[N/m])

For all web wrap angles, the friction coefficient increase rapidly with an increase of roller velocity and it reaches at the value of $\mu \cong 0.3$. After that, in the region of $h_c \le h \le 3\sigma_w$ in the figure, the friction coefficient continuously decreases, and then becomes less than 0.03 for $h>3\sigma_w$. Such a behavior is very similar to that in the Streibek curve, so it may be recognize that the region of $h< h_c$ corresponds to the boundary lubrication region, the region of $h \le h_c \le 3\sigma_w$ corresponds to the mixed lubrication region, and the region of $h>3\sigma_w$ corresponds to the fluid film lubrication region, respectively. As the amount of air diffusion from web surface increases with an increase of web wrap angle, the web spacing decreases. As a result, the boundary and mixed lubrication regions are enlarged, and then the friction coefficient keeps high level for wide range of roller velocity. Good agreements can be seen between the predicted results and the measured data.

Figure 11 shows the relation between the friction coefficient and roller velocity for changing the web tension. The similar behavior as in Figure 10 can be seen in this figure; it is similar to Streibek curve. As the web spacing decreases with an increase of web tension, the boundary and mixed lubrication regions are enlarged, and then the friction coefficient keeps high level for a wide range of roller velocity. The predicted results agree well with the measured data.

Figure 12 shows the relation between the friction coefficient and roller velocity for changing the web width. The behavior in the figure is similar to the Streibek curve as also shown in Figure 10 and 11. As the amount of air leakage from both edges of web increases with a decrease of web width, the web spacing decreases. Then, the boundary and mixed lubrication regions are enlarged and the friction coefficient keeps high level for a wide range of roller velocity. The predicted results agree with the measured data within an allowable errors.

Figure 13 shows the relation between the friction coefficient and roller velocity for changing the roller radius. In this case, the behavior in the figure is also similar to the Streibek curve. The web spacing decreases with a decrease of roller radius, and then the boundary and mixed lubrication regions are enlarged and friction coefficient keeps high level for a wide range of roller velocity.

As shown above, the predicted results of friction coefficient by Eq.(28) agree well with the measured data for changing the five design parameters, web wrap angle, tension, width, roller radius and velocity.

CONCLUSIONS

In this paper, the new theoretical modeling of friction coefficient between the uncoated paper-web and steel roller was presented. The predicted results were compared with the measured data for changing the five design parameters. Good agreements were obtained and the applicability of the prediction model were verified experimentally.

REFERENCES

1. Knox, K.L., and Sweency, T.L., "Fluid Effects Associated with Web Handling," Ind. Eng. Chem. Process Des. Develop., 10-2, 1971, pp. 201-205.
2. Eshel, A., and Elrod, H.G., "The Theory of the Infinitely Wide, Perfectly Flexible, Self-Acting Foil Bearing," Trans. ASME, Journal of Lubr. Technol., 1965, pp. 92-97.
3. Ducotey, K.S., and Good, J.K., "The Importance of Traction in Web Handling," Trans. ASME, Journal of Tibology, 117-4, 1995, pp. 679-684.
4. Ducotey, K.S. and Good, J.K., "The Effect of Web Permeability and Side Leakage on the Air Film Height Between a Roller and Web," Trans. ASME, Journal of Tribology, 120, 1998, pp. 559-565.
5. Rice, B.S., Muftu, S., and Cole, K.A., "A Model for Determining the Asperity Engagement Height in Relation to Web Traction over Non-vented Rollers," Trans. ASME, Journal of Tribology, 124, 2002, pp. 584-564.
6. Hashimoto, H., "Air Film Thekness Estimation in Web Handling Process," Trans. ASME, Journal of Tribology, 121, 1999, pp. 50-55.
7. Hashimoto, H., and Nakagawa, H., "Improvement of Web Spacing and Friction Characteristics by Two Types of Stationary Guides," Trans. ASME, Journal of Tribology, 123, 2001, pp. 509-516.

Theoretical Modeling of Traction Characteristics Between a Paper Web and a Steel Roller Based on the Contact Mechanics

H. Hashimoto, Tokai University, JAPAN

Name & Affiliation	Question
Keith Good Oklahoma State University	You conduct your experiments with the web static and not moving but the roller is moving. How do you know you're not damaging the surface of the web you're trying to study, burnishing the surface during the experiment? It would seem that your test method would affect the asperity heights and thus it is an interfering measurement when attempting to measure traction as affected by air entrapment. You inferred the friction using a measurement of web tension on one side of the test roller and a known web tension (dead weight) on the other side. Did the measured value of web tension from the load cell change through time?
Name & Affiliation	**Answer**
Hiromu Hashimoto Tokai University	I never witnessed a change in the measured web tension during a test..
Name & Affiliation	**Question**
Bob Lucas GL&V USA, Inc.	My question is based on an experience where we had a continuous loop of paper. The fellow conducting the test took the web to a particular speed level. When he generated slippage he couldn't repeat that reading again because once it slipped the material surface of that loop was conditioned and he had to put a new loop in. He had the patience of Job. He did literally hundreds of these loops that were successful tests, which meant there were probably many that were not. To be able to prepare a loop and have a uniform tension and what not sometimes it took several tries to get a good tension distribution. But he did some tests where he would measure friction and to a higher speed and run to a higher speed and run to a higher speed. Then as he took these friction tests, traction tests if you will, at higher speeds then when he slowed back down again, it followed a completely different curve. Thus the paper totally had a different friction as he decreased web velocity from 20 meters a second back down towards 0 meters a second. So it didn't follow anywhere close to the same track as far as effective traction. To follow-up on the question that Dave Roisum raised yesterday and of course what Keith Good has just raised now, there is a serious question in trying to apply this. I'm wondering whether or not the test procedure has contaminated the web?
Name & Affiliation	**Answer**
Hiromo Hashimoto	It's a very important point. I think just now I cannot answer clearly but I will do so in the future.